J. Physiol. (1979), **289**, *pp.* 115–141
With 21 text-figures
Printed in Great Britain

IONIC CURRENTS IN RESPONSE TO MEMBRANE DEPOLARIZATION IN AN APLYSIA NEURONE

BY D. J. ADAMS* AND P. W. GAGE

From the School of Physiology and Pharmacology, University of New South Wales, Kensington 2033, Australia

(*Received 18 May 1978*)

SUMMARY

1. Action potentials recorded in the soma of R_{15} neurones in the abdominal ganglia of *Aplysia juliana* were not suppressed by selective inhibition of either Na or Ca conductance alone. It was necessary to block both conductances to suppress action potentials.

2. Membrane currents generated by step depolarizations of the soma consisted of early transient and delayed steady-state currents. The early transient current could have one or two components depending on the activating depolarization.

3. The early more rapid component had a reversal potential at +54 mV and the reversal potential changed with extracellular Na concentration in accord with the Nernst equation. It was blocked by substitution of impermeant cations for Na, by TTX and by internal injections of Zn. It was concluded that this component was normally a Na current.

4. The later slower component of the transient current had a reversal potential at about +65 mV and the reversal potential changed with extracellular Ca concentration in accord with the Nernst equation. It was blocked by substitution of Mg for Ca or addition of Mn, Co, Ni or verapamil to the extracellular solution. It was concluded that this component was normally a Ca current.

5. Na and Ca currents were generated at different threshold potentials, Na currents first appearing at about −20 mV and Ca currents at −5 to 0 mV.

6. The time-to-peak of both Na and Ca currents was affected by the holding potential, by the amplitude of the activating depolarization, by temperature and by divalent ion concentration.

7. The peak Na and Ca conductances both increased sigmoidally with increasing depolarization, the maximum Na conductance of 10–15 μS being approximately twice the maximum Ca conductance. Peak conductances for Na and Ca reached half-maximum at −8 and +3 mV, respectively.

8. The amplitude of the delayed steady-state current could be varied by changing the extracellular K^+ ion concentration or by adding tetraethylammonium to the extracellular solution. The reversal potential for 'tail currents' was −67 mV and shifted 18 mV when the extracellular K concentration was doubled. It was concluded that the delayed steady-state current was K current.

* Present address: Department of Physiology and Biophysics, University of Washington School of Medicine, SJ-40 Seattle, Washington 98195, U.S.A.

0022-3751/79/2750-0478 $01.50

9. With prolonged depolarizations, K current decayed with a time constant of the order of 1 sec. Peak K conductance increased with increasing depolarization with the half-maximum occurring at a potential more positive than +20 mV. The maximum rate of fractional activation of K conductance was independent of the amplitude of the clamp step.

INTRODUCTION

In squid axons, it is well established that action potentials are caused by a regenerative increase in Na conductance (Hodgkin & Katz, 1949; Hodgkin & Huxley, 1952*a*). It has more recently been found that in some excitable cells an increase in Ca conductance may play a central role in the generation of action potentials (see Hagiwara, 1973; Reuter, 1973). In general the Ca conductance changes elicited by membrane depolarization display a slower time course than Na conductance changes: in particular, the time course of 'inactivation' appears to be slower for Ca than for Na (Geduldig & Gruener, 1970; Okamoto, Takahashi & Yoshii, 1976*a*, *b*; Connor, 1977; Kostyuk & Krishtal, 1977).

Experiments on the giant cell, R_2, of *Aplysia* abdominal ganglia (Frazier, Kandel, Kupferman, Waziri & Coggeshall, 1967) have revealed Na and Ca currents with different time courses and pharmacological properties (Geduldig & Gruener, 1970). Separate Na and Ca channels have also been reported recently in *Helix* neurones using an intracellular dialysis technique (Kostyuk & Krishtal, 1977; Lee, Akaike & Brown, 1977). We have observed distinct separate Na and Ca currents in the cell, R_{15}, in the *Aplysia* abdominal ganglion.

We have studied ionic currents generated by depolarization of the surface membrane of this cell for two main reasons: first to obtain more information about ion channels in excitable membranes in general, and secondly to obtain information about these channels in the neurone R_{15} (Frazier *et al.* 1967) to allow identification of the non-linear displacement currents recorded in the same neurone (Adams & Gage, 1976). The major emphasis has been to characterize Ca currents about which relatively little is known but which are obviously of considerable biological significance, e.g. in excitation–secretion coupling (Katz, 1969; Baker, 1974). Preliminary accounts of some of these results have appeared elsewhere (Adams & Gage, 1976, 1977).

METHODS

Preparation

Specimens of *Aplysia juliana* (wt. 30–150 g) were collected in the coastal waters around Sydney, Australia and kept in a natural sea-water aquarium at 15 °C for periods of up to a month.

The abdominal ganglion was dissected from healthy specimens and pinned to a layer of Sylgard (Dow Corning) in the bottom of a Perspex bath. A ligature was applied to each of the connectives and the nerve cells were exposed by dissecting the connective tissue sheath away from the dorsal surface of the ganglion under a binocular dissecting microscope. The neurone, R_{15} (Frazier *et al.* 1967) which ranged from 120 to 270 μm in diameter, was used in the present experiments.

Solutions

The normal extracellular solution (ASW) contained (m-mole/l.): NaCl, 494; KCl, 11; $CaCl_2$, 11; $MgCl_2$, 19; $MgSO_4$, 30; Tris Cl (tris hydroxymethylaminomethane chloride), 10. Solutions had a pH of 7·7–7·8 at 20 °C. The Tris buffer was made up on the day it was used. Other drugs or ions

(tetrodotoxin (TTX), maculotoxin, tetraethylammonium ions, manganese, cobalt, nickel and zinc) were also addded to solutions immediately before use. Maculotoxin was a crude extract (Croft & Howden, 1972) from the posterior salivary glands of the octopus, *Hapalochlaena maculosa*. When ions were added in sufficient concentration to increase significantly the osmotic pressure of solutions, the concentration of NaCl was lowered to compensate. Solutions were continuously bubbled with air and flowed through the tissue bath (2·5 ml.) at a rate of 3 ml./min. Bath temperature, controlled by circulating refrigerated fluid through a water jacket around the bath, was monitored by a thermistor probe placed close to the ganglion and could be controlled to within 0·5 °C in the range 4–25 °C.

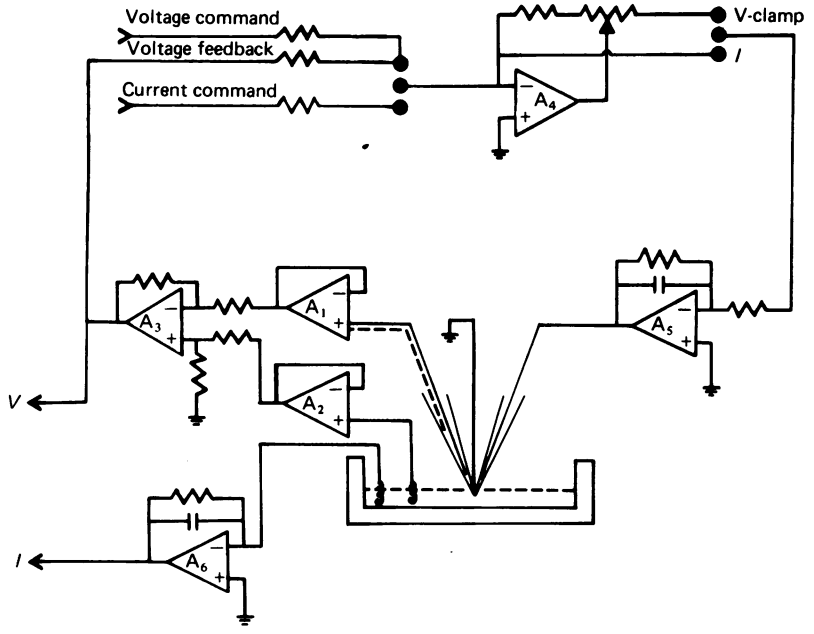

Fig. 1. Circuit for voltage clamping the soma of R_{15} and measuring membrane currents. A_1, picometric amplifier with capacity neutralization; A_2, unity gain follower (Philbrick 1009); A_3, differential amplifier; A_4, clamping amplifier (Philbrick P45A). The feed-back loop contains a 1 MΩ variable resistor giving a gain adjustable from 0 to 10^3 with an output voltage maximum of ± 15 V; A_5, voltage amplifier (Philbrick 1022): fixed gain of ten with maximum output voltage of ± 140 V (time constant 3 μsec/100 V); A_6, current monitor. Current flow was recorded across a 1 kΩ resistor.

Recording techniques and equipment

Conventional glass micro-electrodes were used to record membrane potential and to pass current. For monitoring membrane potential, electrodes were filled with 3 M-KCl and had resistances of 5–7 mΩ. Current-passing electrodes were filled with 2 M-K citrate, or a mixture of K citrate (1·8 M) and KCl (0·8 M), and had resistances of 2–5 MΩ. The bath was connected via a 3 M-KCl–agar electrode and Ag–$AgCl_2$ junction positioned 'downstream' from the ganglion to an operational amplifier (Philbrick 1011) in ammeter configuration effectively grounding the bath (Gage & Eisenberg, 1969). The feed-back loop consisted of 1 kΩ and 1 nF in parallel.

For voltage clamping, a voltage-recording micro-electrode and a current-passing micro-electrode were inserted into a cell with an angle of approximately 60° between them (Eisenberg & Engel, 1970). Membrane potential was recorded differentially between the intracellular micro-electrode and an extracellular electrode similar to, but separate from, the bath ground electrode. The intracellular electrode was connected to a Picometric amplifier (Instrumentation Laboratory Inc.) with capacity neutralization. The circuit used is shown in Fig. 1. The capacity neutralization was adjusted by applying a small step of current across the voltage-recording electrode and increasing the capacity neutralization until the recorded voltage change had a

rise time of 10–20 μsec. This also allowed electrode resistance to be measured. In order to prevent 'ringing', the rise time of command voltage steps was slowed to 5–30 μsec and the gain of the feed-back was slowly increased using the 1 MΩ variable resistor (Fig. 1). To reduce capacitive coupling between the electrodes, an aluminium shield connected to ground was placed between

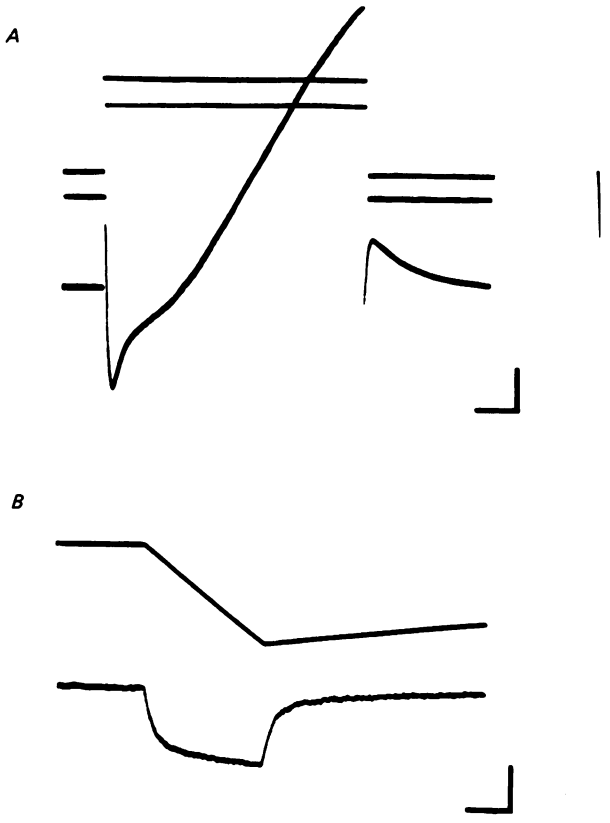

Fig. 2. *A*, spatial control of voltage-clamped soma membrane. The two upper records show membrane potential monitored independently from separate micro-electrodes located within the soma. The lower of the two voltage traces monitors the membrane potential 'used' in the voltage-clamp circuit. The bottom trace shows the membrane current generated by the depolarization. Holding potential, −45 mV. Temp. 16 °C. Calibration: vertical, 20 mV (upper traces), 200 nA (lower trace); horizontal, 10 msec. *B*, membrane area was determined approximately (see Methods) by imposing a ramp change of V_m (upper trace, $dV/dt = 7{\cdot}8\ V.sec^{-1}$) and recording the current flow across the membrane (lower trace). The slow, time-dependent change in the current trace is probably due to changes in the K^+ ion concentration adjacent to the cell membrane. Calibration: vertical, 100 nA for current, 10 mV for voltage; horizontal, 1 msec.

the voltage-recording and current-passing micro-electrodes and lowered to within about 0·5 mm of the surface of the neurone. Capactitive loss of current from the current-passing electrode to the bath was minimized by lowering the bath solution to within 0·5 mm of the surface of the neurone also. The lower edge of the shield was insulated to prevent electrical contact with the solution. The time constant of the recording system was reduced by 'driving' the shield of the wire connecting the voltage micro-electrode to the input amplifier. In some experiments a driven metal sleeve was placed around the current micro-electrode also, but generally this was found not to be necessary. Voltages and currents were displayed on an oscilloscope (Tektronix 565) and photographed. In some experiments a minicomputer (PDP 81, Lab 8 system) was used to average signals.

Spatial control of membrane potential

In order to confirm that the membrane potential of the soma of cells was indeed well controlled under voltage clamp, in several experiments a second voltage-recording electrode was inserted into the soma of R_{15}, equidistant from the other two electrodes. It was found that the membrane potential recorded with this third electrode was within 5% of that recorded with the other voltage electrode over the whole range of clamp potentials. A record illustrating this is shown in Fig. 2. Some recent observations (Roberge, Jacob, Gulrajani & Mathieu, 1977) indicate that the interior of R_{15} is isopotential during an action potential so that it seems reasonable to assume isopotentiality under voltage clamp conditions also.

It was not possible to measure membrane potential in the axon of R_{15} but obviously it would be possible to voltage clamp only a short length of the axon. However, in the present studies the axon was ligated about 300–400 μm from the soma. This was done in an attempt to minimize the contribution of currents from the axon which would not be space-clamped. Even so, some of the currents recorded under voltage clamp could be arising in imperfectly clamped patches of membrane in the stump of axon but this was believed to be only a small fraction of the total current because of the relative membrane areas. For example, in other *Aplysia* neurones when the membrane current from a small patch of soma was compared with the total current (for depolarizations greater than 20 mV) the two currents were found to have identical time courses (see figs. 2 and 3 in Frank & Tauc, 1964). We found in R_{15} that, with small depolarizing pulses (< 20 mV), there was sometimes a delay in the onset of a Na current which may have originated in the axon stump. However, a similar delay was not seen with Ca currents even when there was no Na current obscuring their onset, perhaps because little or no Ca current is generated in the axon: there is some reason to believe that Ca currents would be generated only in the soma of R_{15}. In Na-free solutions the axon (further than 250 μm from the soma) is electrically inexcitable (Wald, 1972; Junge & Miller, 1974; Standen, 1975; Horn & Miller, 1977) suggesting that there is no self-regenerative increase in Ca conductance in the distal axon.

On the whole then, it was thought that the Na currents measured in response to depolarizations greater than 20 mV, and Ca currents at all potentials, provided accurate representations of the underlying conductance changes in the soma membrane.

Series resistance

The resistance in series with the membrane was determined as described by Moore & Cole (1963). Measurements of the total series resistance (R_s) were obtained either from $\Delta V/\Delta I$ where ΔV is the size of the initial jump in the voltage transient in response to a brief current step, ΔI, or from the time course of the capacitive current generated by a hyperpolarizing pulse (Hodgkin, Huxley & Katz, 1952). R_s was found to be 1–2 kΩ in the larger cells used in these experiments, approximately 0·1% of the membrane resistance. No compensation was made for this series resistance. The difference between true and recorded membrane potential ($= I_m.R_s$, where I_m is the current flow across the membrane) would have been less than 2 mV during the largest inward Na or Ca currents.

Rate of change of membrane potential

The time constant of change in membrane potential (τ_c) in response to a voltage step can be calculated (Katz & Schwartz, 1974) using the equation $\tau_c = C_o R_o R_s/R_o + R_s$, where R_o and C_o are the 'input' resistance and capacitance respectively, and R_s is the series resistance. As R_o was much larger than R_s, $\tau_c \simeq R_o C_o$. In sixteen neurones, the average value of C_o was 17·5 nF giving an average τ_c of considerably less than 100 μsec. In no neurone was the calculated τ_c greater than 150 μsec.

Leakage current

To correct for leakage current, the steady-state leakage conductance G_l was determined with hyperpolarizing steps and assumed to be constant within the range of membrane potentials studied (Hodgkin, *et al.* 1952; see also Adelman & Taylor, 1961). Certainly for hyperpolarizing steps up to 100 mV the relationship between current and voltage was ohmic in R_{15}. Only results from experiments in which the leakage current for a 100 mV hyperpolarizing pulse was less than 40 nA (corresponding to $G_l < 0{\cdot}4$ μS) are described.

Estimation of membrane area

A voltage ramp was applied to the membrane (under voltage clamp) to obtain an estimate of the effective membrane area (Armstrong, 1969). The total capacitive current, I_c, is given by $I_c = C_c.dV/dt$. For a linearly varying potential the capacitive current generated by a voltage ramp should be constant and give a measure of C_c (Fig. 2). Assuming a membrane capacity of 1 μF/cm^2, which seems a reasonable value for cell membranes (Cole, 1968), the membrane area estimated from C_c was found to be in the range 0·012–0·022 cm^2. Hence the currents in R_{15} can be multiplied by 40–90 to obtain mean current densities per cm^2. Because of uncertainties about

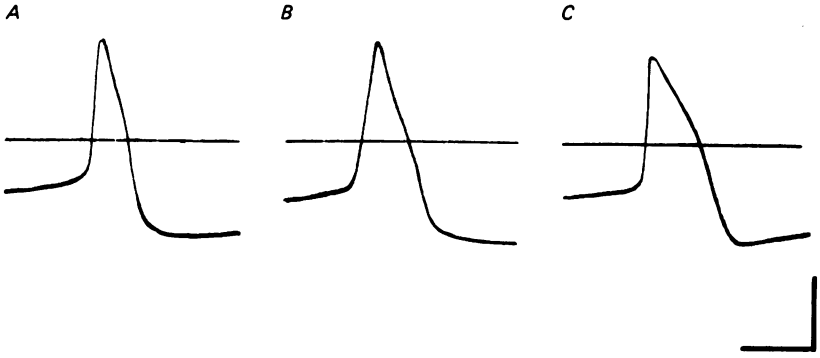

Fig. 3. Action potentials recorded from the neurone R_{15} in *A*, normal ASW; *B*, Na-free (Tris substitution) ASW; and *C*, Ca-free (Mg substitution) ASW. Resting membrane potential −44 mV. Temp. 18 °C. Calibrations: vertical, 40 mV; horizontal, 20 msec.

active membrane area and the spatial distribution of channels, results have not been expressed here as current densities however. The calculated membrane area was approximately ten times as large as the surface area of a sphere of the same diameter. This is probably due to extensive infolding of the soma membrane seen in electron micrographs (Andrews, 1977) so that the true surface area is much larger than that of a sphere of equivalent diameter. A similar morphological explanation has been offered before to account for high values of apparent specific membrane capacitance obtained in molluscan neurones (Gorman & Mirolli, 1972; Graubard, 1975).

RESULTS

Na—Ca action potentials

The neurone R_{15} spontaneously generates action potentials from a resting potential of about −40 mV. One of these action potentials in normal 'artificial sea water' (ASW) is shown in Fig. 3*A*. When Tris, choline or sucrose was substituted isosmotically for Na^+ ions, action potentials persisted. An action potential recorded in Na-free ASW containing Tris as Na substitute, is shown in Fig. 1*B*. Similarly, when Ca^{2+} ions were removed from the extracellular solution (Mg^{2+} ions substituted for Ca^{2+} ions) action potentials could still be recorded (Fig. 3*C*). Only when both Na^+ and Ca^{2+} ions were replaced by impermeable substitutes in the extracellular solution could action potentials not be evoked. Total replacement of external Na by either choline or Tris decreased the overshoot of action potentials by several millivolts and the maximum rate of rise (dV/dt) was consistently decreased to about half its normal value. It was also noticed that, in Ca-free solutions, the rate of repolarization of action potentials was decreased.

From these results it was concluded that there is a regenerative increase in both

Na and Ca conductance in the surface membrane of R_{15}, as has been demonstrated in R_2 (Junge, 1967; Geduldig & Junge, 1968). These ions could conceivably be passing through one channel or through two separate channels. The following experiments were done in an attempt to distinguish between these two possibilities.

Ionic currents in voltage-clamped neurones

Currents generated by depolarization of the surface membrane of R_{15} normally consisted of a transient inward current followed by a delayed sustained outward current (Fig. 4). With voltage steps to membrane potentials more positive than

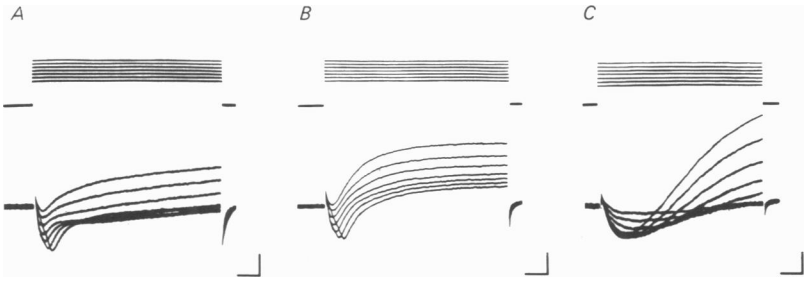

Fig. 4. Membrane currents (lower traces) generated by depolarizing voltage-clamp steps (upper traces) in test solutions containing TEA ions (25 mM). *A*, normal ASW. *B*, ASW containing Mn^{2+} ions (15 mM). *C*, Na-free (choline substitution) ASW. Holding potential −42 mV. Temp. 8·5 °C. Calibrations: *A* and *B*, vertical, 50 mV (voltage traces), 200 nA (current traces); horizontal, 10 msec. *C*, vertical, 50 mV (voltage traces), 100 nA (current traces); horizontal, 20 msec.

−5 mV, the transient inward current appeared to consist of two temporally distinct components, an early, more rapidly decaying current followed by a late slower, smaller current (Fig. 4*A*). When Mn^{2+} ions (15 mM) were added to the extracellular solution, the later, slower component disappeared (Fig. 4*B*). On the other hand in a Na-free solution (choline substituted for Na), the early more rapid inward current disappeared, leaving a slow inward current (Fig. 4*C*). Such experiments demonstrated that it was possible to dissect the inward current into two components, an early Na current and a later Ca current.

The early transient current

The amplitude of the early transient current depended on the concentration of Na^+ ions in the extracellular solution. The peak amplitude of this current plotted against membrane potential is shown in Fig. 5 (temp. 10 °C). The currents were recorded in ASW containing NaCl in concentrations of 444 mM (circle), 247 mM (squares) and 165 mM (triangles). The reversal potentials for the early transient currents were +54, +42 and +32 mV respectively in these three solutions. If this current is carried only by Na^+ ions, the reversal potential of +54 mV in a solution containing 444 mM-Na would indicate a free intracellular Na concentration of 48·5 mM. If the intracellular Na concentration remained constant as the extracellular concentration was changed, reversal potentials of +40 and +30 mV would be predicted in solutions containing 247 and 165 mM-Na, respectively. These are very

close to the observed reversal potentials of +42 and +32 mV indicating that the early transient current is indeed a Na current.

Another observation supporting the conclusion that the early transient current is a Na current, is the effect of TTX which selectively blocks Na channels in excitable

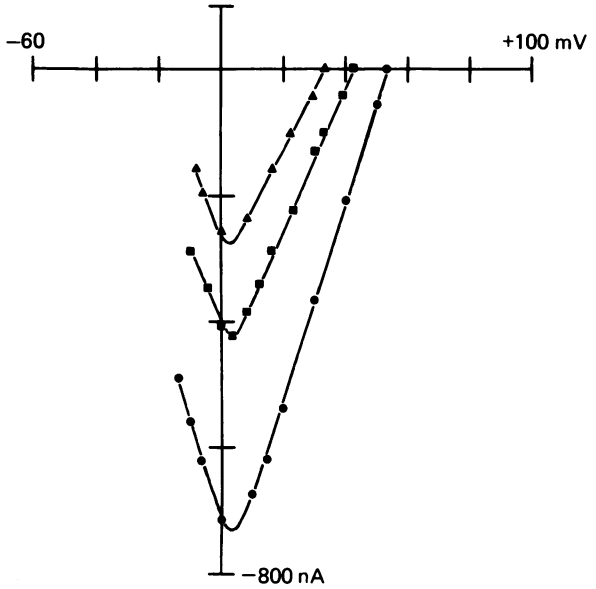

Fig. 5. Effect of Na concentration on Na currents. Peak amplitudes of early transient inward currents obtained during 60 msec pulses are plotted against clamp potential. Current–voltage curves are shown for 444 mM-Na (circles), 247 mM-Na (squares) and 165 mM-Na (triangles) ASW. Holding potential, −48 mV. Temp. 12 °C. (Leakage conductance 0·35 μS.)

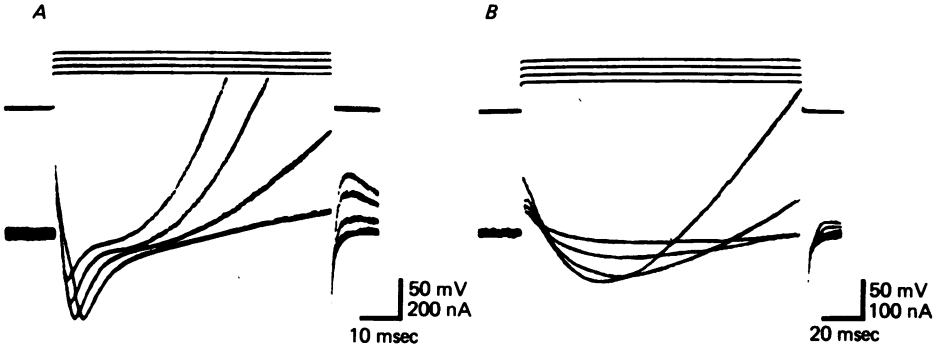

Fig. 6. Membrane currents recorded in normal ASW (*A*) and in ASW containing 3×10^{-5} M-TTX (*B*). Upper traces show voltage steps; lower traces show clamp currents. Holding potential −45 mV. Temp. 10 °C. Calibrations: vertical, 50 mV for voltage, 200 nA for current in *A*, 100 nA for current in *B*; horizontal, 10 msec in *A*, 20 msec in *B*.

membranes (Narahashi, Moore & Scott, 1964). When R_{15} was exposed to normal ASW containing TTX at concentrations from 10^{-5} to 3×10^{-5} M, the early transient current was completely blocked but the later transient and delayed currents were unaffected (Fig. 6). The early transient current was also inhibited by maculotoxin (MTX; 10^{-5} g/ml.), which has been shown to block selectively the Na current in

squid axons (Gage, Moore & Westerfield, 1976). Unlike TTX, the effectiveness of MTX in reducing the early transient current amplitude was dependent upon the rate of repetitive depolarization which is consistent with the observations on the effect of MTX in skeletal muscle fibres and squid axons (Dulhunty & Gage, 1971; Gage *et al.* 1976). MTX did not affect significantly the late transient current nor the delayed outward current, confirming its selectivity for the Na channel.

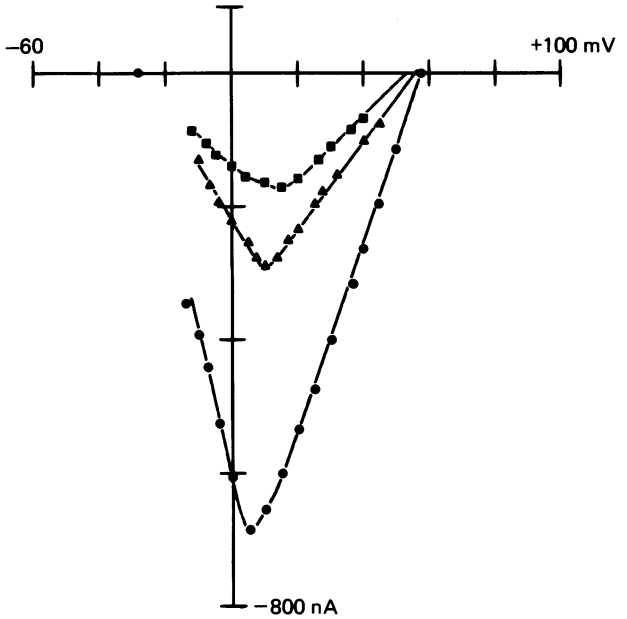

Fig. 7. Inhibition of Na current by Zn injection. Ionophoretic injection of Zn produced marked depression of the inward Na current. The peak of early inward currents is plotted against clamp potential before Zn injection (circles) and after injecting Zn^{2+} for 10 min (triangles) and 30 min (squares). The Zn injection caused a shift in the peak of the *I–V* curves to the right but there was no great change in the reversal potential. External solution: normal ASW containing 50 mM-TEA. Leakage conductance increased from 0·4 μS (control) to 0·75 μS after 30 min of Zn injection. Holding potential, −50 mV. Temp. 10·5 °C.

In three experiments, the effect of internal injection of Zn, which is known to depress Na ionic and 'gating' currents (Begenisich & Lynch, 1974; Armstrong & Bezanilla, 1974) was examined. Ionophoretic injection of Zn irreversibly reduced the amplitude of Na currents. The depression of the early transient current in one of these experiments is shown in the current–voltage curves in Fig. 7. The Zn injection caused a shift in the maximum current to more positive potentials and there was a small change (about 5–6 mV) in the reversal potential.

In summary, the shifts in reversal potential with changes in extracellular Na concentration, and the effects of TTX, MTX and internal Zn which selectively block Na currents in excitable membranes, strongly indicate that the early transient current passes through a Na channel.

Replacement of Na by Li, Cs or K

When Na^+ ions in the external solution were replaced by Tris or choline, the early transient currents disappeared, as shown in Fig. 4*C*. In contrast, the Na channel was clearly permeable to Li^+ ions. Replacement of all the external Na by Li did not change significantly the time course nor the reversal potential for the early transient current but caused a reduction in its amplitude. Current–voltage plots obtained from a cell in Na-ASW and Li-ASW are shown in Fig. 8. The peak amplitude of the early

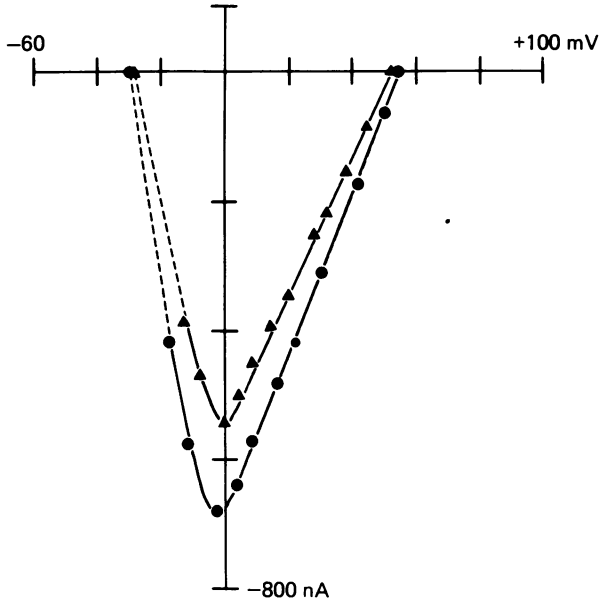

Fig. 8. *I–V* curves for the early transient current in Na (circles) and Li (triangles) ASW. Na and Li currents were recorded in Ca-free (Mg substitued) solutions containing either Na (494 mM) or Li (494 mM). Holding potential, −46 mV. Temp. 31 °C.

transient current at 0 mV was approximately 20% smaller in Li-ASW than in Na-ASW presumably because of a decrease in channel conductance. The addition of 10^{-5} M-TTX to Li-ASW blocked this Li current. This strongly supports the assumption that Li ions pass through the Na channel.

Within five to six minutes' exposure to Cs-ASW no early inward currents in response to depolarizing clamp steps were observed, as shown in Fig. 9, whereas neither the later inward nor the delayed outward currents were essentially altered in Cs-ASW. Early outward currents could be seen with clamp steps to potentials more positive than 0 mV but these were not systematically studied. It was noticed that the potassium 'tail' current following repolarization to the holding potential was blocked in Cs-ASW (Fig. 9). Extracellular Cs has also been reported to reduce inward rectification by blocking K channels in R_2 (Eaton & Brodwick, 1976) and in starfish egg cell membrane (Hagiwara, Miyazaki & Rosenthal, 1976).

In three experiments external Na was replaced by K^+ ions. K-ASW depolarized the surface membrane (V_m = −5 to +5 mV) and there was a marked increase in the

leakage conductance. In order to discern the ionic currents more easily, currents in response to equal hyperpolarizing and depolarizing pulses from the holding potential were averaged. No early inward currents were clearly detectable in K-ASW with clamp pulses more positive than 0 mV although later transient currents still occurred. This indicated that the shift in the reversal potential for current through the Na channel was greater than 54 mV.

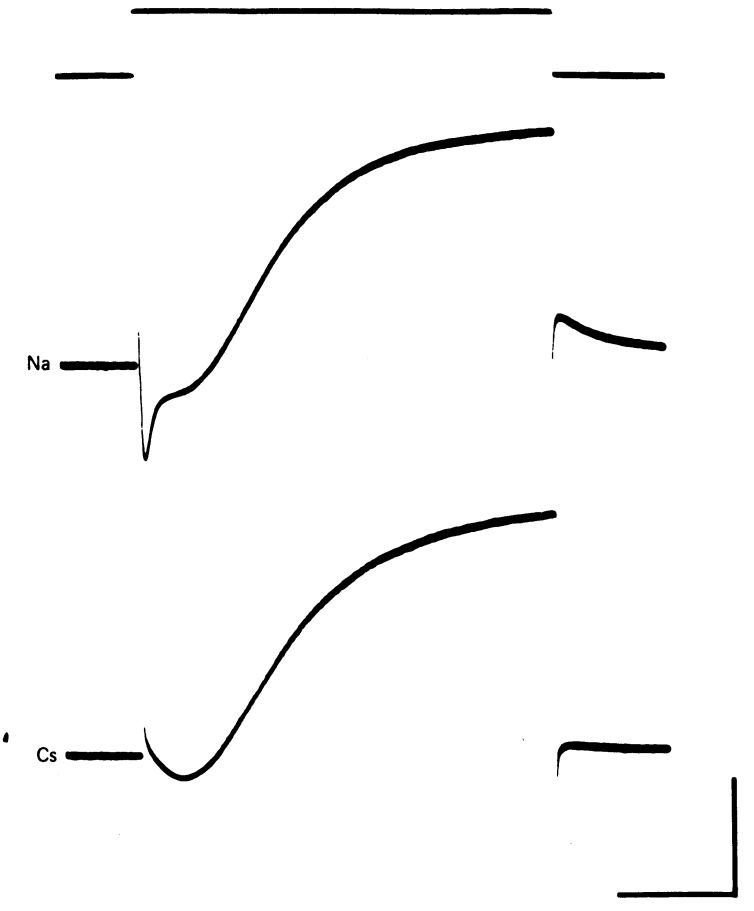

Fig. 9. Clamp currents in Na and Ca solutions in response to the voltage step (54 mV) in the top trace. Replacement of Na by Cs in the external solution abolished the early inward current indicating that the Na channel is relatively impermeable to Cs^+ ions. Holding potential, −46 mV. Temp. 12·5 °C. Note the rate of decay of the K tail current is markedly changed in the presence of external Cs^+ ions. Calibration: vertical, 100 mV (top trace), 1 μA (current traces); horizontal, 40 msec.

From these results, it was concluded that the Na channel was permeable to Na^+ and Li^+ ions but relatively impermeable to Cs^+ and K^+ ions, as has been found in other excitable membranes (Chandler & Meves, 1965; Hille, 1972; Okamoto *et al.* 1976*a*).

The late transient current

The late transient current was recorded in solutions containing no Na^+ ions or TTX (or both) so that the early transient current was suppressed. Tetraethylammonium (TEA) was also added to inhibit the delayed outward current. In such solutions the amplitude and time course of the late transient current could be measured accurately at potentials more negative than about +60 mV. At potentials more positive than +60 mV a small delayed outward current appeared in spite of the presence of 70 mm-TEA and it became difficult to have confidence in measurements which required subtraction of this current (Fig. 10*B*). In spite of these difficulties, it was possible to measure the reversal potential of the late inward current with reasonable accuracy.

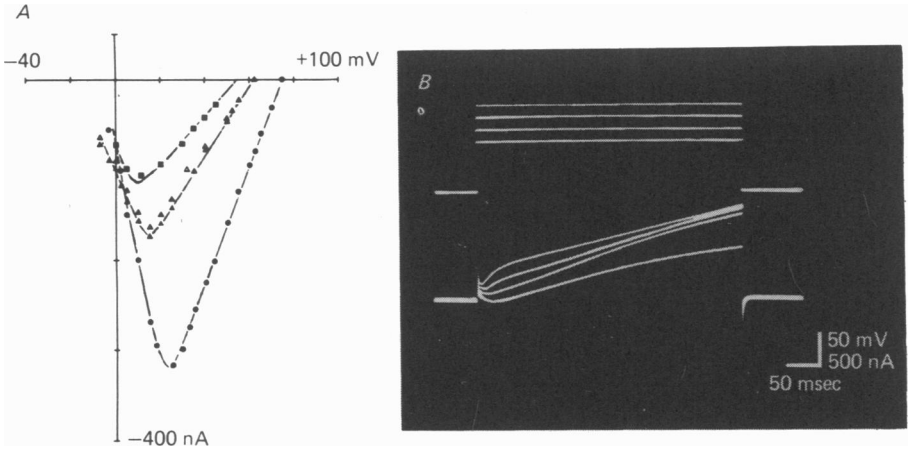

Fig. 10. *A*, effect of varying external Ca concentration on current–voltage curves of peak inward Ca current against clamp potential. Records were obtained in Na-free (choline substituted) ASW containing 70 mM-TEA at external Ca concentrations of 5 mM (squares), 11 mM (triangles) and 55 mM (circles). Leakage conductance 0·3 μS (increased in reduced calcium ASW). Holding potential, −44 mV. Temp. 11·5 °C. Note the shift to the right of the *I–V* curve on increasing the extracellular Ca concentration. *B*, reversal of inward Ca current with depolarizing steps to potentials more positive than +65 mV. Ionic currents were recorded in Na-free (choline substitution) ASW containing 10^{-5} M-TTX and 25 mM-TEA. Holding potential, −40 mV. Temp. 10 °C. Calibrations: vertical, 50 mV for voltage, 500 nA for current; horizontal, 50 msec.

Current–voltage curves for late transient currents recorded in solutions containing 55 mM-Ca^{2+} (circles), 11 mM-Ca^{2+} (triangles) and 5 mM-Ca^{2+} (squares) are shown in Fig. 10*A* and the reversal potentials (from extrapolation) were +75, +63 and +54 mV respectively. Assuming that the reversal potential gives the Ca equilibrium potential, an intracellular Ca concentration of 6×10^{-5} M was calculated from the equilibrium potential of +63 mV in 11 mM-Ca^{2+} (temp. 10 °C). From this, reversal potentials of +83 and +56 mV would be predicted in solutions containing 55 and 5 mM-Ca^{2+}, respectively. The reasonable agreement between observed and predicted values supports the hypothesis that the late inward current is carried by Ca^{2+} ions.

It is interesting that the *I–V* curves (Fig. 10*A*) shifted to the right with increasing

Ca concentration. This observation is consistent with the proposal (Frankenhaeuser & Hodgkin, 1957; Hille, 1968; Hille, Woodhull & Shapiro, 1975) that Ca^{2+} ions, by binding to or 'shielding' negatively-charged membrane sites, affect the electrical field 'seen' by voltage sensors of ionic channels.

The late transient current could be depressed selectively by adding Mn^{2+} ions to the ASW (Fig. 11*A*; (see also Fig. 4*B*). Depression of the late transient current

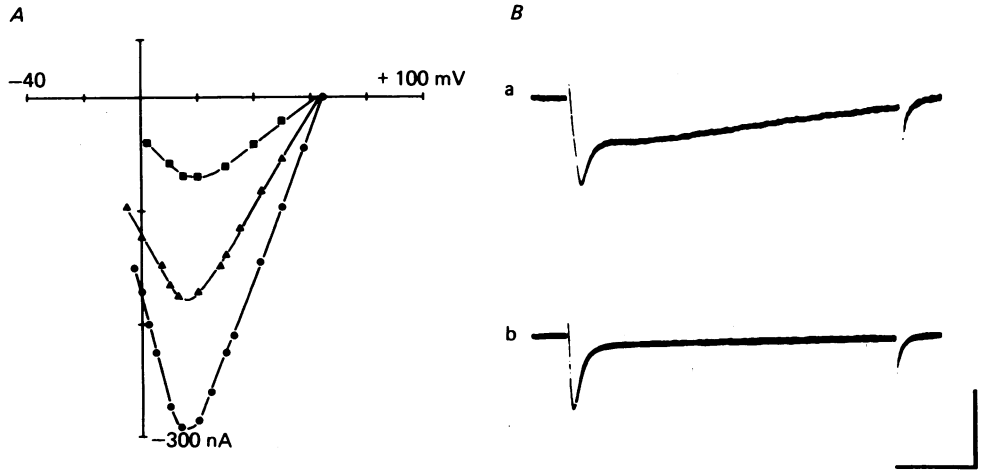

Fig. 11. *A*, current–voltage curves of the peak inward Ca current in control solution (circles) and in the presence of 5 mM (triangles) and 10 mM (squares) Mn^{2+} ions. Increasing the extracellular Mn concentration depressed Ca currents and produced a slight shift in the peak of the *I–V* curve to the right. There was no significant change in the reversal potential. Holding potential, −40 mV. Leakage conductance 0·2 μS. Temp. 12·5 °C. *B*, inward currents recorded in normal ASW (top trace) and in a Ca-free (Mg substituted) ASW (bottom trace) were obtained with a clamp pulse to +20 mV from a holding potential of −40 mV. Solutions contained 50 mM-TEA. Temp. 10 °C. Calibration: vertical, 400 nA; horizontal 40 msec.

became progressively greater as Mn concentration was increased and was reversible on return to control solutions. As can be seen from the current–voltage curves in Fig. 11*A*, late transient currents were reduced 42 and 78 % in solutions containing 5 mM (triangles) and 10 mM (squares) Mn respectively, when compared with the late transient current in control solution (circles). It can be seen from Fig. 11*A* that Mn caused no significant change in the reversal potential of the late transient current. Zinc (1–5 mM), Co (10–30 mM) and Ni (5–15 mM) were found to inhibit competively the late transient current also.

The late transient current disappeared when Mg^{2+} ions were substituted for Ca^{2+} ions (Fig. 11*B*), or when no Ca was added to extracellular solutions. In the latter case, the threshold potential for eliciting Na currents shifted several millivolts to more negative potentials and there was an increase in leakage conductance. The disappearance of the late transient current on removal of Ca from the extracellular solution provides further evidence that this current is normally carried by Ca ions.

Verapamil (0·25 mM), an organic Ca antagonist (Kohlhardt, Bauer, Krause & Fleckenstein, 1972) was found to be effective in blocking the late transient current

but also reduced the Na current. A similar non-selective action of verapamil has been reported in squid axons (Baker, Meves & Ridgway, 1973) and in crayfish muscle (Van der Kloot & Kita, 1975).

In the light of the inhibitory effects of divalent ions recognised as Ca current inhibitors, the dependence on extracellular Ca^{2+} ions and the suppressing effect of verapamil, it was concluded that the late transient current was normally a Ca current.

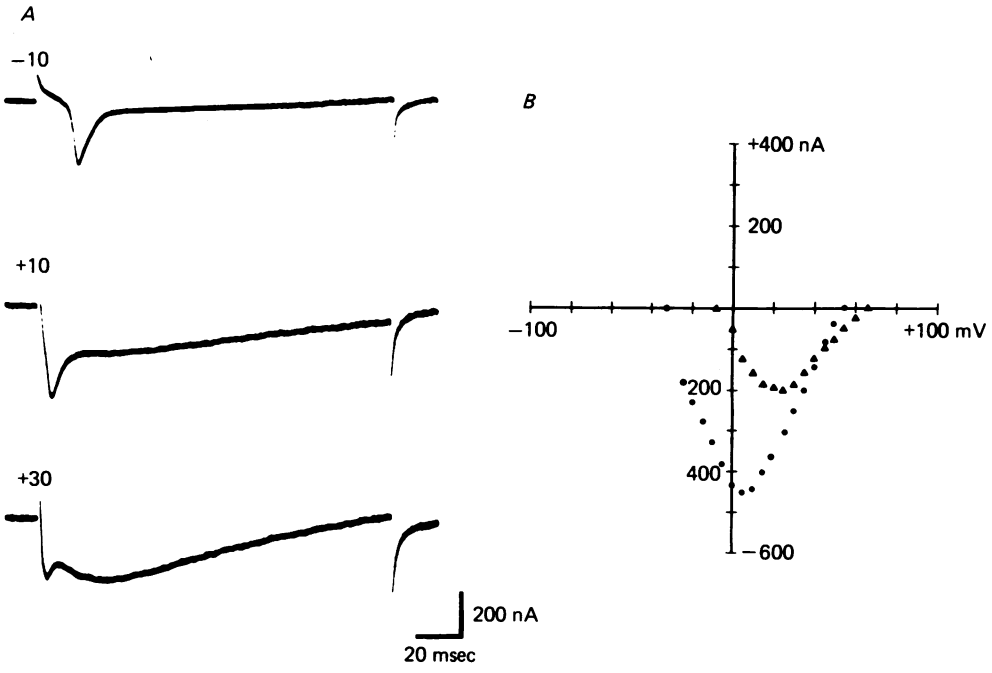

Fig. 12. Difference in threshold potential for Na and Ca currents. *A*, inward currents obtained in normal ASW containing 50 mM-TEA at clamp potentials of −10, +10 and +30 mV. Calibration: vertical, 200 nA; horizontal, 20 msec. *B*, peak amplitudes of Na (circles) and Ca (triangles) currents plotted as a function of membrane potential. Na currents were recorded in ASW containing 15 mM-Mn, Ca currents in Na-free ASW (choline substitution). Holding potential −40 mV. Temp. 8·5 °C.

Na and Ca currents have different thresholds

As the neurone R_{15} was progressively depolarized with voltage steps from the resting membrane potential, an early inward current was first seen at membrane potentials of −20 to −10 mV. This current (top trace of Fig. 12*A*) had the properties of the Na current described above. With larger depolarizing steps (Fig. 12*A*), the later, slower Ca current could be clearly seen, usually first becoming detectable with voltage steps to −5 to 0 mV. Typical ionic currents recorded at clamp potentials of −10, +10 and +30 mV in the presence of 50 mM-TEA are shown in Fig. 12*A*.

In order to obtain current–voltage curves for the Na and Ca currents in the same experiment, the preparation was first exposed to Na-free ASW (choline substitution) to allow measurement of Ca currents, then to ASW containing the normal Na concentration and Mn^{2+} ions (15 mM) to allow measurement of Na currents. Current–

voltage curves obtained in this way are shown in Fig. 12*B* for Na current (circles) and Ca current (triangles). The graph clearly demonstrates the difference in threshold, amplitude and reversal potential of the Na and Ca currents. Calcium currents were generated at more positive potentials, were smaller in amplitude and had a more positive reversal potential than Na currents. The potentials at which the Na and Ca channels were activated could be most clearly differentiated when the holding potential was set at potentials at which Na conductance was inactivated (Adams & Gage, 1979). For example, at a holding potential of −18 mV, clamp steps to more positive potentials activated only the Ca current.

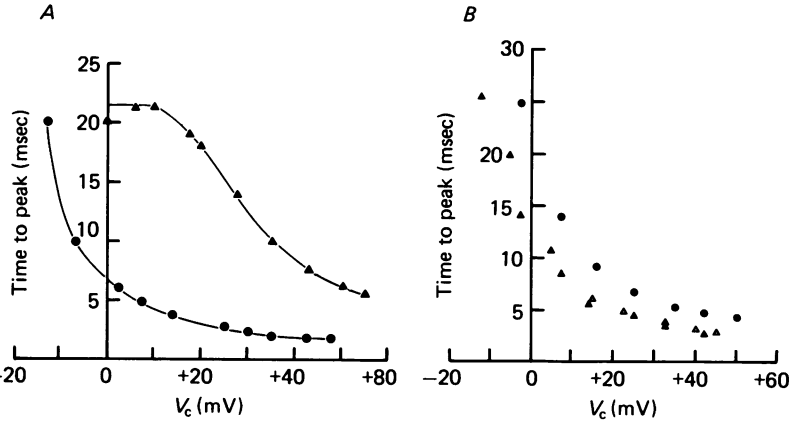

Fig. 13. *A*, effect of membrane potential on the time-to-peak of Na and Ca currents. Time-to-peak of Na currents (circles) was obtained in normal ASW containing 15 mM-Mn and 50 mM-TEA, while the time-to-peak of Ca currents (triangles) was obtained in Na-free (choline substituted) ASW containing 10^{-5} M-TTX and 50 mM-TEA. Holding potential −45 mV. Temp. 13·5 °C. *B*, effect of holding potential (V_H) on the time-to-peak of Na currents recorded in normal ASW containing 50 mM-TEA. On shifting the holding potential from −42 mV (filled triangles) to a more negative potential of −102 mV (filled circles) the time-to-peak increased at all clamp potentials. The effect was reversed on return to a V_H of −42 mV (open triangles). Temp. 9 °C.

Time course of Na and Ca currents

The time-to-peak of Na currents was generally shorter than the time-to-peak of Ca currents. For both currents, the time-to-peak was reduced at more depolarized potentials. These observations are illustrated graphically in Fig. 13*A* in which time-to-peak for Na (circles) and Ca (triangles) currents are plotted against clamp potential (holding potential −45 mV, temp. 13·5 °C).

The time-to-peak of both Na and Ca currents was also found to be affected by temperature, holding potential and divalent cation concentration. In the range 8–20 °C, the average Q_{10} values of the time-to-peak of Na and Ca currents were 2·6 and 3·1 (two experiments), respectively. Holding potential also had a clear effect on the time-to-peak of Na current as shown in Fig. 13*B*. With a holding potential of −42 mV (triangles) the time-to-peak of Na currents was less at any clamp potential than when the holding potential was −102 mV (circles). This effect was completely reversible and not due to deterioration of the preparation. The filled triangles in

Fig. 13*B* were obtained from records before, and the open triangles from records after, the holding potential was changed to −102 mV. A similar effect of holding potential on the time-to-peak of Ca currents was also seen.

The effect of extracellular Ca concentration on the time-to-peak of Na and Ca currents is illustrated in Fig. 14. Raising the Ca concentration from 11 to 55 mM

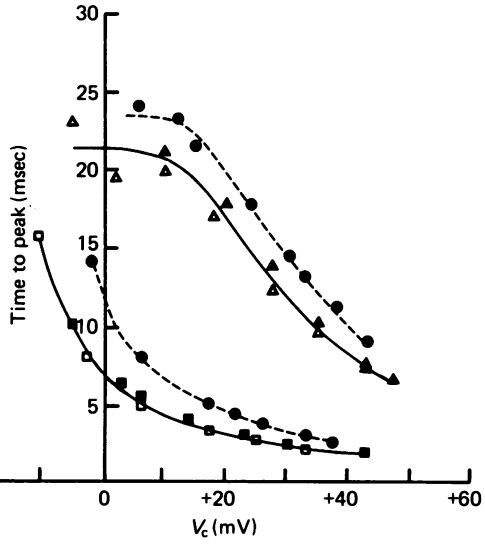

Fig. 14. Effect of extracellular Ca concentration on the time-to-peak of Na and Ca currents. Na currents were recorded in 11 mM-Ca^{2+} (filled squares) and 55 mM-Ca^{2+} (circles) ASW external solutions containing 50 mM-TEA. Holding potential, −45 mV. Temp. 10·5 °C. Ca currents were recorded in 11 mM-Ca^{2+} (filled triangle) and 55 mM-Ca^{2+} (filled circles), Na-free (choline substituted) ASW containing 50 mM-TEA. Holding potential −42 mV. Temp. 12 °C. Recovery of both Na and Ca currents in 11 mM-Ca^{2+} is shown by the open squares and triangles, respectively.

increased the time-to-peak of both currents over the whole range of clamp potentials and the effect was reversible. The percentage change in time-to-peak was considerably less for the Ca currents than for the Na currents.

Zinc also affected the time-to-peak of Na currents. At concentration of 1–5 mM in the external solution, Zn reversibly increased the time-to-peak of Na currents at all potentials as shown in Fig. 15. Similar effects of extracellular Zn on the time-to-peak of Na currents have been observed in other excitable cells (Blaustein & Goldman, 1968; Armstrong & Bezanilla, 1975).

Peak Na and Ca conductance as a function of membrane potential

The potential dependence of the peak Na (G_{Na}) and Ca (G_{Ca}) conductances was measured in normal and Na-free solutions, respectively. The peak conductances were calculated according to the equations $G_{Na} = I_{Na}/(V_c - \epsilon_{Na})$ and $G_{Ca} = I_{Ca}/(V_c - \epsilon_{Ca})$, where I_{Na} and I_{Ca} are peak Na and Ca currents, ϵ_{Na} and ϵ_{Ca} are measured Na and Ca reversal (equilibrium) potentials, and V_c is clamp potential. Peak values of both Na and Ca conductance increased sigmoidally as the membrane was depolarized (Fig. 16). The graph shows that the maximum peak Na conductance was greater

than the maximum peak Ca conductance. It can also be seen that half-maximum peak conductance occurred at about −8 mV for Na and at about +3 mV for Ca. As will be shown in the following paper (Adams & Gage, 1979) both the rates of activation and the rates of inactivation of Na and Ca conductance are affected by membrane

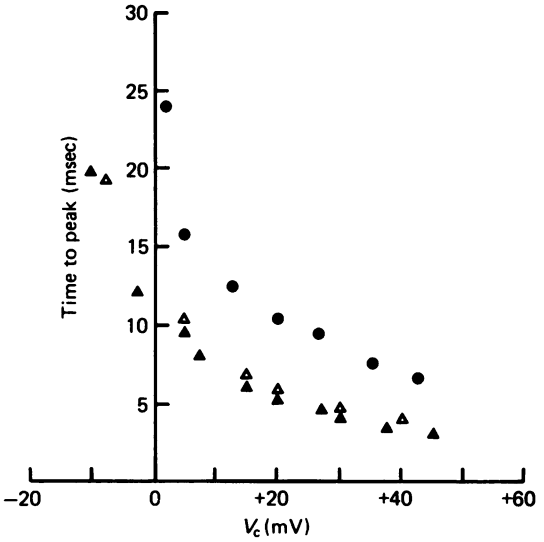

Fig. 15. Effect of extracellular Zn on the time-to-peak of Na currents. Na currents were recorded in normal ASW containing 50 mM-TEA (filled triangles) and then in a solution containing 1 mM-Zn (filled circles). The effect was reversed on return to control solution (open triangles). Holding potential, −44 mV. Temp. 11·5 °C.

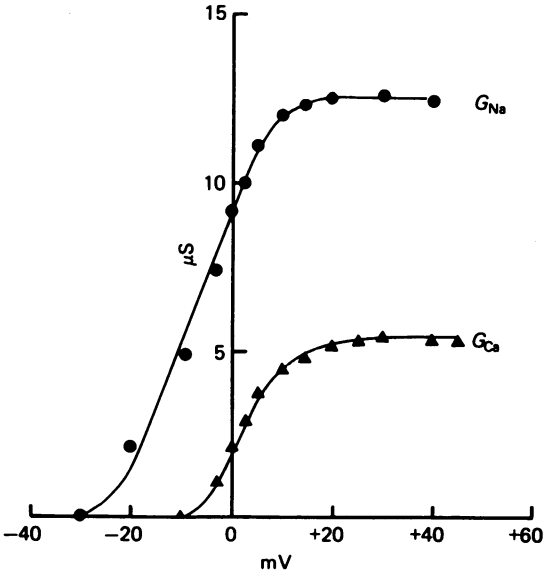

Fig. 16. Peak Na (G_{Na}, circles) and Ca (G_{Ca}, triangles) conductances as a function of membrane potential. G_{Na} and G_{Ca} were determined from the peak amplitude of Na and Ca currents obtained in normal and Na-free ASW external solutions, respectively in the same cell. Holding potential, −45 mV. Temp. 12·5 °C. Midpoints of the conductance–voltage curves are −8 mV for G_{Na} and +3 mV for G_{Ca}.

potential so that the voltage dependence of these peak conductances cannot be simply interpreted. However, the graph does serve to illustrate the marked differences in the potential required to 'turn-on' the two types of conductance and in the maximum peak conductances.

The maximum peak amplitudes of both Na and Ca conductance were sensitive to temperature and had a Q_{10} of 2 in the range 8–20 °C. Again as both the rates of activation and inactivation are temperature sensitive, this result is also difficult to interpret simply.

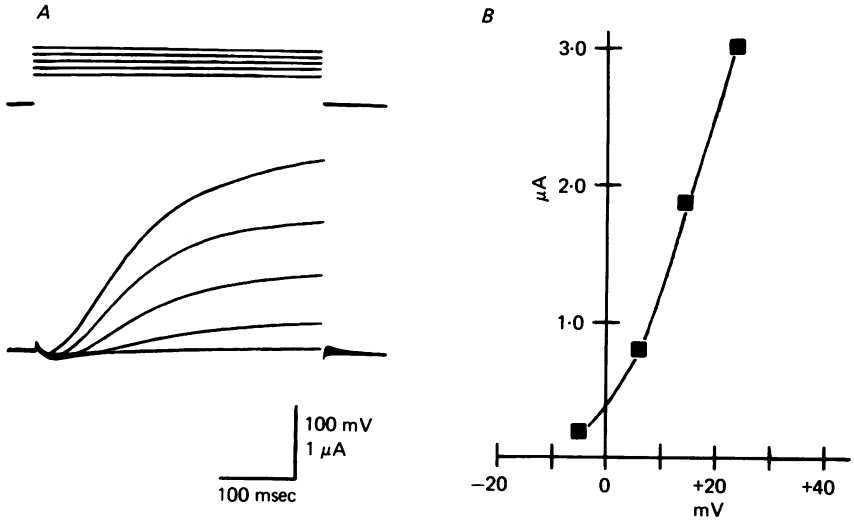

Fig. 17. Effect of membrane potential on delayed steady-state currents generated by depolarizing steps from a holding potential of −42 mV. Records were obtained in a Na-free (choline substitution) ASW containing 11 mM-Ca and 10^{-5} M-TTX. *A*, currents (lower traces) generated by depolarizing pulses (upper traces). Temp. 10 °C. Calibrations: vertical, 100 mV for voltage, 1 μA for current; horizontal, 100 msec. *B*, the peak amplitude of steady-state currents is plotted against membrane potential.

The delayed outward current is K current

The delayed outward current which was activated by depolarizing pulses to potentials more positive than −30 mV had a sigmoid rising phase and then formed a plateau for several hundred milliseconds (Fig. 17*A*). The amplitude of the current varied with membrane potential as shown in the current–voltage curve in Fig. 17*B*. It is clear from the *I–V* curve that the equilibrium potential for the ion (or ions) moving across the membrane during the delayed outward current would be more negative than −10 mV. The likely candidates would be K^+ or Cl^- ions. The amplitude of the current varied with extracellular K concentration, but did not change when NO_3^- ions were substituted for Cl^- ions in the extracellular solution. Nor did the amplitude change when sucrose was substituted for NaCl. It seemed likely, therefore, that the outward current was carried mainly by K^+ ions. If so, the reversal potential for the delayed current should be at the K equilibrium potential.

On the assumption that the conductance increase responsible for the delayed outward current would take some time to relax following repolarization after a

depolarizing pulse, 'tail currents' generated in this way were examined to determine the potential at which the direction of the tail current reversed. Relatively small, brief depolarizing command pulses were used to activate the delayed conductance to avoid shifts of the equilibrium potential due to extracellular ion accumulation adjacent to the cell membrane (Alving, 1969; Eaton, 1972; Neher & Lux, 1973). One of these experiments is illustrated in Fig. 18. The membrane potential was stepped to

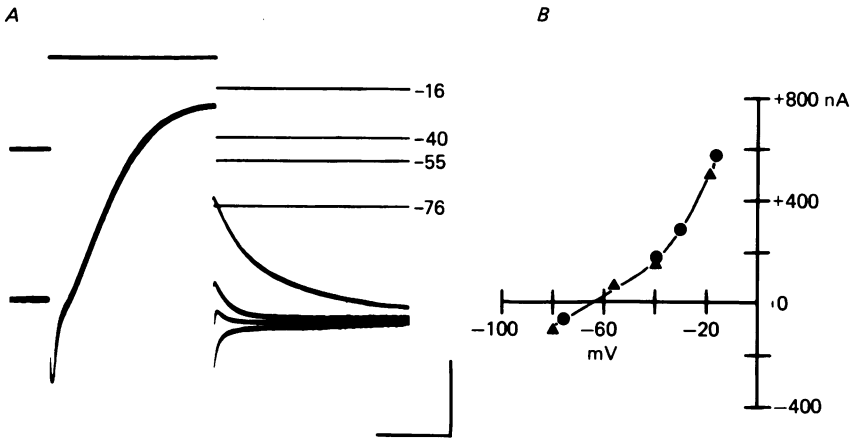

Fig. 18. Effect of membrane potential on K tail currents. *A*, tail currents were elicited by repolarization at the peak of the delayed outward current to different levels of membrane potential. Membrane currents were generated in normal ASW from a holding potential of −48 mV. Temp. 12·5 °C. Calibration: vertical, 40 mV (voltage traces), 400 nA (current traces); horizontal, 100 msec. *B*, amplitude of tail currents plotted against the level of membrane potential stepped back to (two cells). Reversal potentials for tail currents were determined from such graphs.

a depolarized level to activate the delayed outward current. During successive trials, the membrane potential was stepped back to levels of −16, −40, −55 and −76 mV and it can be seen that the tail current reversed between −55 and −76 mV. In this experiment in normal (11 mM-K) ASW the reversal potential of the tail currents was found to be at −66 mV. In a total of three experiments, the reversal potential of tail currents was -67 ± 3 mV (S.E. of mean). These values are reasonably close to an ϵ_K value of −75 mV measured in R_{15} with K-selective electrodes (A. M. Brown, personal communication). Increasing the external K concentration twofold (22 mM-K-ASW) in this experiment shifted the tail current reversal potential by 18 mV to −48 mV. Because the reversal potential of the tail current was in the vicinity of ϵ_K and the shift in reversal potential when the external K concentration was changed was close to that predicted for a K-selective electrode, it was concluded that the delayed current was due to an increase in K conductance. Further evidence for this conclusion is provided by the depressant effect of TEA ions on the delayed current, described below.

Voltage dependence of the K conductance

K conductance (G_K) plotted as function of membrane potential in normal ASW is shown in Fig. 19. The K conductance generated by a depolarizing clamp pulse

(V_c) was calculated assuming a passive 'ohmic' channel, with $G_K = I_K/(V_c - e_K)$, where I_K is the peak K current amplitude and e_K is the K equilibrium potential (measured from tail currents). The K conductance curve was studied up to a membrane potential of +50 mV. Results obtained in three neurones are shown in Fig. 19

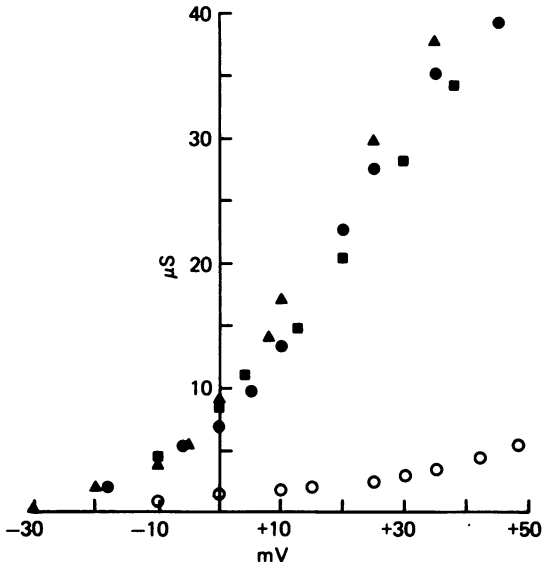

Fig. 19. Depression of K conductance by TEA. Peak K conductance (G_K) is plotted against clamp potential. G_K was calculated from the peak amplitude of delayed outward currents generated by depolarizing clamp steps of 500–600 msec duration. Filled circles: Na-free ASW, holding potential (V_H) of −42 mV, temp. 10 °C; filled squares: Na-free ASW, V_H −45 mV, temp. 8 °C; filled triangles: normal ASW, V_H −46 mV, temp. 9 °C; open circles: Na-free ASW containing 25 mM-TEA. Note the depression of G_K in the external solution containing 25 mM-TEA. Results shown by circles were obtained in the same cell.

(filled symbols). At +50 mV, the K conductance had obviously not reached a maximum; it can be seen that half maximum G_K must occur at a potential more positive than +20 mV. The conductance at +50 mV was approximately 40 μS, about three times the maximum Na conductance.

TEA depresses the delayed K conductance

Externally applied TEA ions which have been shown to inhibit K currents in nerve membranes selectively (for reviews see Hille, 1970; Armstrong, 1975), reversibly depressed K conductance in R_{15}. The effect of 25 mM-TEA on K conductance is shown in Fig. 19. Potassium conductance in control solution (filled circles) was clearly depressed by TEA (25 mM, open circles). These measurements (circles) were made in the same cell. It was found that 50% depression of G_K could be obtained with 5–10 mM-TEA in the extracellular solution. In 50 mM-TEA, G_K was reduced to less than 5% of normal. Although depressing the amplitude of G_K significantly, TEA did not appear to affect its rate of 'turn-on'.

Effect of membrane potential on the rate of activation of K conductance

To describe the effect of membrane potential on the time course of the K conductance, the maximum rate of rise of the latter (dG_K/dt) was determined during a clamp step. As shown in Fig. 20*A*, dG_K/dt increased as the amplitude of depolarizating pulses was increased as has been described for K conductance in squid axon

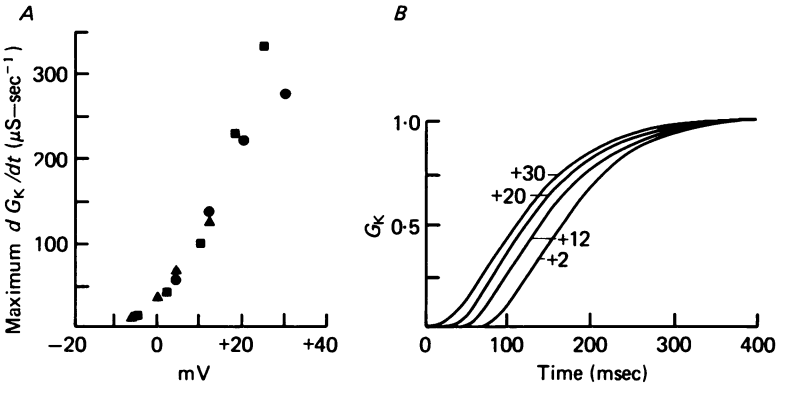

Fig. 20. Effect of membrane potential on the rate of activation of K conductance. *A*, maximum dG_K/dt plotted against membrane potential. Data were obtained in Na-free ASW; circles: V_H −42 mV; triangles: V_H −44 mV, and in normal ASW; squares: V_H −45 mV, temp. 14 °C. *B*, K conductance, expressed as a fraction of the maximum steady-state conductance, plotted against time, for four clamp potentials (+30, +20, +12 and +2 mV). Temp. 10 °C. Note the decrease in the delay of onset of activation with increasing depolarization.

(Hodgkin & Huxley, 1952*a*). This increase in dG_K/dt with depolarization could be due either to an increase in the rate of activation of K conductance or to an increase in the final (steady-state) number of channels activated by depolarization. To distinguish between these two possibilities, K conductance was plotted as a fraction of the maximum K conductance at that potential (G_K, Fig. 20*B*). As shown in Fig. 20*B* the rate of activation then appears to be voltage-independent but the delay in activation of the K conductance is, in contrast, markedly voltage-dependent (Cole & Moore, 1960).

Time-dependent depression of K currents

During a prolonged depolarizing clamp pulse, the delayed outward current slowly declined in amplitude with time following an approximately exponential time course. The decline of outward K current during a 3 sec depolarizing clamp pulse is shown in Fig. 21. Here the time constant of decay was 1·25 sec (clamp potential −3 mV, temperature 12 °C). Although 'inactivation' of K currents with long-duration clamp pulses has been reported in some molluscan neurones (Connor & Stevens, 1971*a*; Kostyuk, Krishtal & Doroshenko, 1975*a*) the decline of the outward K currents recorded in the present experiments could be partly due to accumulation of K in the extracellular solution at the membrane surface. In fact, in *Aplysia* pacemaker

neurones it has been suggested that K accumulation is the most important component of the time-dependent depression of K currents (Alving, 1969; Eaton, 1972). Any underlying real inactivation of K conductance would be obscured if the large K currents which flow during large depolarizations cause K accumulation in the extracellular space as the K equilibrium potential would change with time, giving an apparent change in conductance.

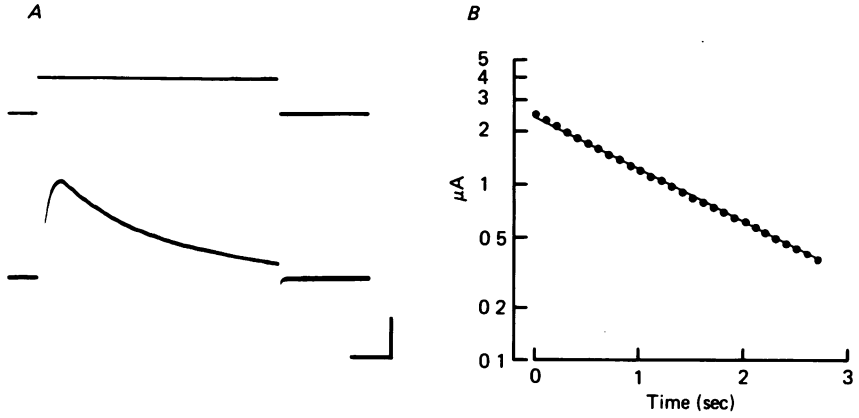

Fig. 21. Depression of the delayed outward K current during a maintained depolarizing clamp pulse. *A*, outward K current generated by depolarizing to −3 mV for 3 sec (normal ASW). Holding potential, −45 mV. Temp. 12 °C. Calibration: vertical, 50 mV (upper trace), 1 μA (lower trace); horizontal, 500 msec. *B*, semilogarthmic plot of the outward K current against time during the decay. The decline of the K current from the peak is exponential with a time constant of 1·25 sec.

DISCUSSION

The main aim in these experiments was to establish the existence of and to identify two separate, transient, (normally inward) currents generated by depolarization of the surface membrane of the neurone R_{15} in *Aplysia* abdominal ganglia. It has been shown that these currents have different properties and normally consist of an early, more rapid Na current followed by a later, slower Ca current. They can be separated by their different time courses, thresholds, reversal potentials, susceptibility to ion substitutions, and sensitivity to recognised specific blocking agents such as TTX and Mn^{2+} ions. The results presented confirm and extend the hypothesis of separate Na and Ca channels in the molluscan soma membrane reported previously in R_2 (Geduldig & Gruener, 1970) and in *Helix* neurones (Kostyuk & Krishtal, 1977).

The differential sensitivity of the two currents to blocking agents indicates that there are two separate 'channels', one selective for Na^+ ions and the other for Ca^{2+} ions. The 'Na channel' is also permeable to Li^+ ions but relatively impermeable to Cs^+ or K^+ ions. The 'Ca channel' is permeable to Sr^{2+} and Ba^{2+} ions also, but less so than to Ca^{2+}, as determined from reversed potential measurements (D. J. Adams & P. W. Gage, unpublished observations).

A clear and useful distinguishing characteristic of Na and Ca currents in R_{15} is the difference in the level of depolarization required to activate them (Fig. 12). This has

not been seen in other molluscan neurones (Standen, 1975; but see Fig. 4, Kostyuk & Krishtal, 1977). It will be shown in a later paper (Adams & Gage, 1979, in the press) that the difference in the potentials for activation of Na and Ca currents is reflected in similar threshold differences for Na and Ca 'gating' currents.

Although the existence of separate Na and Ca currents is clear, it is possible that their time course or amplitude could have been affected by other ionic currents generated by membrane depolarization. Two currents which might do this have been described in other molluscan neurones: an early transient K current (Hagiwara, Kusano & Saito, 1961; Connor & Stevens, 1971*b*; Neher, 1971; Faber & Klee, 1972; Kostyuk *et al.* 1975*a*; Thompson, 1977) might distort the transient Na and Ca currents and a Ca-dependent K curret (Meech & Standen, 1975; Heyer & Lux, 1976; Thompson, 1977) might distort the later time course of the Ca current (and the depolarization-activated K current). We think that the recorded Na and Ca currents were not significantly distorted in this way for the following reasons. The transient K current that has been recorded with depolarizing steps only from relatively hyperpolarized holding potentials is depressed by TEA (Connor & Stevens, 1971*b*; Kostyuk, Krishtal & Doroshenko, 1975*b*; Thompson, 1977). With holding potentials at the resting or more positive potentials there should have been no transient K current. In most of the experiments described here, holding potentials more positive than -50 mV were used. Furthermore, solutions generally contained TEA which should have depressed any early transient K current. With regard to a Ca-activated K current, the 'turn-on' of such a current could conceivably accelerate the decay of the Ca current. High concentrations of TEA were used in most solutions in an attempt to depress both this and the depolarization-activated K currents. The best evidence that the time course of the Ca current is not significantly contaminated by a Ca-activated K current in solutions containing TEA is given in the following paper (Adams & Gage, 1979): the decay of the amplitude of Ca tail currents with time follows the time course of decay of the underlying Ca current.

The Ca equilibrium potential of $+63$ mV measured from the reversal potential of Ca currents was lower than expected and would predict an intracellular Ca concentration of approximately 6×10^{-5} M (10 °C) which seems rather high (but see Hencek & Zachar, 1977). A possible source of error which might have given low values for ϵ_{Ca} could be progressive depression of the amplitude of Ca currents by Ca-dependent outward K currents with increasing depolarization. However, the shifts in ϵ_{Ca} with changes in extracellular Ca concentration were in accord with predictions from the Nernst equation and are not easy to reconcile with such an explanation. In addition, the onset of a K current would have had to be very rapid to affect the peak amplitude of Ca currents. And finally, solutions contained TEA which depresses Ca-dependent K currents (Meech & Standen, 1975; Thompson, 1977). We do not think therefore that the Ca currents contained a significant component of K current, at least at potentials more negative than about $+60$ mV. Another possibility is that the inward Ca currents produced an intracellular accumulation of Ca^{2+} ions in an unstirred layer adjacent to the membrane so that the measured ϵ_{Ca} does not reflect the Ca concentration in the bulk of the intracellular solution.

The maximum peak amplitude of Na currents (seen at -5 to 0 mV) was of the order of $5–8 \times 10^{-7}$ A, corresponding to a peak conductance of about 10–15 μS (5–15 °C). For a cell with a total surface area of about 0·02 cm^2 (see Methods) an upper figure for Ca current density of approximately 40 μA.cm^{-2} and for membrane conductance of approximately 1 mS.cm^{-2} can be calculated from the peak current. These values are considerably less than for Na current density and conductances in squid axons (Hodgkin & Huxley, 1952*b*). However, these calculations are based on the assumption that Na channels are uniformly distributed over the surface mem-

brane. In fact, channel density may be lower in the infoldings of the cell than on the surface. Other explanations for the lower Na conductance of the *Aplysia* nerve cell membrane could be that there is a lower density of Na channels or a lower single channel conductance in the surface membrane of R_{15} than in squid axon membrane.

The peak Ca current in Na-free ASW was maximal at +10 to +15 mV. The peak value of $3–5 \times 10^{-7}$ A (5–15 °C) gives a Ca conductance of about 5–10 μS. Taking a total membrane area of the order of 0·02 cm^2 into account as before, the maximum Ca current density would be about 25 μA.cm^{-2} and the maximum membrane conductance approximately 0·5 mS.cm^{-2} at the peak of the Ca current. This specific Ca conductance in R_{15} is similar to the value of 0·7 mS.cm^{-2} obtained for specific Ca conductance in barnacle muscle fibres (Keynes, Rojas, Taylor & Vergara, 1973). The relatively high values for Ca conductance and low values for Na conductance indicate that regenerative Ca conductance probably plays an important role in the generation of action potentials in the soma of R_{15}.

In conclusion, depolarization of the surface membrane of the soma of R_{15} activates two separate transient ion channels, one selective for Na^+ ions and the other for Ca^{2+} ions. These two types of channels open with very different kinetics, presumably reflecting different voltage-dependent conformation changes in membrane proteins.

The work was supported by a grant from the Australian Research Grants Committee. We are grateful to R. Malbon, P. Holtz and C. Prescott for technical assistance.

REFERENCES

ADAMS, D. J. & GAGE, P. W. (1976). Gating currents associated with sodium and calcium currents in an *Aplysia* neuron. *Science, N.Y.* **192**, 783–784.

ADAMS, D. J. & GAGE, P. W. (1977). Calcium channel in *Aplysia* nerve cell membrane: ionic and gating current kinetics. *Proc. Aust. physiol. pharmacol. Soc.* **8**, 28*P*.

ADAMS, D. J. & GAGE, P. W. (1979). Characteristics of sodium and calcium conductance changes produced by membrane depolarization in an *Aplysia* neurone. *J. Physiol.* **289**, 143–161.

ADAMS, D. J. & GAGE, P. W. (1979). Sodium and calcium gating currents in an *Aplysia* neurone. *J. Physiol.* (in the press).

ADELMAN, W. J. & TAYLOR, R. E. (1961). Leakage current rectification in the squid giant axon. *Nature, Lond.* **190**, 883–885.

ALVING, B. O. (1969). Differences between pacemaker and nonpacemaker neurons of *Aplysia* on voltage clamping. *J. gen. Physiol.* **54**, 512–531.

ANDREWS, S. (1977). A study of neurones in *Aplysia* abdominal ganglia. M.Sc. thesis, University of New South Wales, Sydney.

ARMSTRONG, C. M. (1969). Inactivation of the potassium conductance and related phenomena caused by quaternary ammonium ion injections in squid axons. *J. gen. Physiol.* **54**, 553–575.

ARMSTRONG, C. M. (1975). Ionic pores, gates and gating currents *Quart.Rev. Biophys.* **7**, 179–210.

ARMSTRONG, C. M. & BEZANILLA, F. (1974). Charge movement associated with the opening and closing of the activation gates of the Na channels. *J. gen. Physiol.* **63**, 533–552.

ARMSTRONG, C. M. & BEZANILLA, F. (1975). Currents associated with the ionic gating structures in nerve membrane. *Ann. N.Y. Acad. Sci.* **264**, 265–277.

BAKER, P. F. (1974). Excitation-secretion coupling. *Recent Advances in Physiology*, **9**, 51–86.

BAKER, P. F., MEVES, H. & RIDGWAY, E. B. (1973). Effects of manganese and other agents on the calcium uptake that follows depolarization of squid axons. *J. Physiol.* **231**, 511–526.

BEGENISICH, T. & LYNCH, C. (1974). Effects of internal divalent cations on voltage-clamped squid axons. *J. gen. Physiol.* **63**, 675–689.

BLAUSTEIN, M. P. & GOLDMAN, D. E. (1968). The action of certain polyvalent cations on the voltage-clamped lobster axon. *J. gen. Physiol.* **51**, 279–291.

CHANDLER, W. K. & MEVES, H. (1965). Voltage clamp experiments on internally perfused giant axons. *J. Physiol.* **180**, 788–820.

COLE, K. S. (1968). *Membranes, Ions and Impulses.* Berkeley: University of California Press.

COLE, K. S. & MOORE, J. W. (1960). Potassium ion current in the squid giant axon: dynamic characteristic. *Biophys. J.* **1**, 1–14.

CONNOR, J. A. (1977). Time course separation of two inward currents in molluscan neurones. *Brain Res.* **119**, 487–492.

CONNOR, J. A. & STEVENS, C. F. (1971*a*). Inward and delayed outward membrane currents in isolated neural somata under voltage clamp. *J. Physiol.* **213**, 1–20.

CONNOR, J. A. & STEVENS, C. F. (1971*b*). Voltage clamp studies of a transient outward membrane current in gastropod neural somata. *J. Physiol.* **213**, 21–30.

CROFT, J. A. & HOWDEN, M. E. H. (1972). Chemistry of maculotoxin: a potent neurotoxin isolated from *Hapalochlaena maculosa*. *Toxicon* **10**, 645–651.

DULHUNTY, A. & GAGE, P. W. (1971). Selective effects of an octopus toxin on action potentials. *J. Physiol.* **218**, 433–445.

EATON, D. C. (1972). Potassium ion accumulation near a pace-making cell of *Aplysia*. *J. Physiol.* **224**, 421–440.

EATON, D. C. & BRODWICK, M. S. (1976). Inward rectification in *Aplysia* giant neurons. *Biophys. J.* **16**, 24a.

EISENBERG, R. S. & ENGEL, E. (1970). The spatial variation of membrane potential near a small source of current in a spherical cell. *J. gen. Physiol.* **55**, 736–757.

FABER, D. S. & KLEE, M. R. (1972). Membrane characteristics of bursting pacemaker neurones in *Aplysia*. *Nature New Biol.* **240**, 29–31.

FRANK, K. & TAUC, L. (1964). Voltage-clamp studies of molluscan neuron membrane properties. In *The Cellular Function of Membrane Transport*, ed. HOFFMAN, J. F., pp. 113–135. Englewood Cliffs, New Jersey: Prentice Hall.

FRANKENHAEUSER, B. & HODGKIN, A. L. (1957). The action of calcium on the electrical properties of squid axons. *J. Physiol.* **137**, 218–243.

FRAZIER, W. T., KANDEL, E. R., KUPFERMAN, I., WAZIRI, R. & COGGESHALL, R. E. (1967). Morphological and functional properties of identified neurons in the abdominal ganglion of *Aplysia californica*. *J. Neurophysiol.* **30**, 1288–1351.

GAGE, P. W. & EISENBERG, R. S. (1969). Capacitance of the surface and transverse tubular membrane of frog sartorius muscle fibres. *J. gen. Physiol.* **53**, 265–278.

GAGE, P. W., MOORE, J. W. & WESTERFIELD, M. (1976). An octopus toxin, maculotoxin, selectively blocks sodium current in squid axons. *J. Physiol.* **259**, 427–443.

GEDULDIG, D. & GRUENER, R. (1970). Voltage clamp of the *Aplysia* giant neurone: early sodium and calcium currents. *J. Physiol.* **211**, 217–244.

GEDULDIG, D. & JUNGE, D. (1968). Sodium and calcium components of action potentials in the *Aplysia* giant neurone. *J. Physiol.* **199**, 347–365.

GORMAN, A. L. F. & MIROLLI, M. (1972). The passive electrical properties of the membrane of a molluscan neurone. *J. Physiol.* **227**, 35–50.

GRAUBARD, K. (1975). Voltage attenuation within *Aplysia* neurons: the effect of branching pattern. *Brain Res.* **88**, 325–332.

HAGIWARA, S. (1973). Ca spike. *Adv. Biophys.* **4**, 71–102.

HAGIWARA, S., KUSANO, K. & SAITO, N. (1961). Membrane changes of *Onchidium* nerve cell in potassium-rich media. *J. Physiol.* **155**, 470–489.

HAGIWARA, S., MIYAZAKI, S. & ROSENTHAL, N. P. (1976). Potassium current and the effect of caesium on this current during anomalous rectification of the egg cell membrane of a starfish. *J. gen. Physiol.* **67**, 621–638.

HENČEK, M. & ZACHAR, J. (1977). Calcium currents and conductances in the muscle membrane of the crayfish. *J. Physiol.* **268**, 51-71.

HEYER, C. B. & LUX, H. D. (1976). Control of the delayed outward potassium currents in bursting pacemaker neurones of the snail, *Helix pomatia*. *J. Physiol.* **262**, 349–382.

HILLE, B. (1968). Charges and potentials at the nerve surface: divalent ions and pH. *J. gen. Physiol.* **51**, 221–236.

HILLE, B. (1970). Ionic channels in nerve membranes. *Prog. Biophys. molec. Biol.* **21**, 1–32.

HILLE, B. (1972). The permeability of the sodium channel to metal cations in myelinated nerve. *J. gen. Physiol.* **59**, 637–658.

HILLE, B., WOODHULL, A. M. & SHAPIRO, B. I. (1975). Negative surface charge near sodium channels of nerve: divalent ions, monovalent ions, and pH. *Phil. Trans. R. Soc.* B **270**, 301–318.

HODGKIN, A. L. & HUXLEY, A. F. (1952*a*). Currents carried by sodium and potassium ions through the membrane of the giant axon of *Loligo*. *J. Physiol.* **116**, 449–472.

HODGKIN, A. L. & HUXLEY, A. F. (1952*b*). A quantitative description of membrane current and its application to conduction and excitation in nerve. *J. Physiol.* **117**, 500–544.

HODGKIN, A. L., HUXLEY, A. F. & KATZ, B. (1952). Measurement of current–voltage relations in the membrane of the giant axon of *Loligo*. *J. Physiol.* **116**, 424–448.

HODGKIN, A. L. & KATZ, B. (1949). The effect of sodium ions on the electrical activity of the giant axon of the squid. *J. Physiol.* **108**, 37–77.

HORN, R. & MILLER, J. J. (1977). A prolonged, voltage-dependent calcium permeability revealed by tetraethylammonium in the soma and axon of *Aplysia* giant neuron. *J. Neurobiol.* **8**, 399–415.

JUNGE, D. (1967). Multi-ionic action potentials in molluscan giant neurones. *Nature, Lond.* **215**, 546–548.

JUNGE, D. & MILLER, J. (1974). Different spike mechanisms in axon and soma of molluscan neurone. *Nature, Lond.* **252**, 155–156.

KATZ, B. (1969). *The Release of Neural Transmitter Substances*. Liverpool: University Press.

KATZ, G. M. & SCHWARTZ, T. L. (1974). Temporal control of voltage-clamped membranes: an examination of principles. *J. Membrane Biol.* **17**, 275–291.

KEYNES, R. D., ROJAS, E., TAYLOR, R. E. & VERGARA, J. (1973). Calcium and potassium systems of a giant barnacle muscle fibre under membrane potential control. *J. Physiol.* **229**, 409–455.

KOHLHARDT, M., BAUER, B., KRAUSE, H. & FLECKENSTEIN, A. (1972). Differentiation of the transmembrane Na and Ca channels in mammalian cardiac fibres by the use of specific inhibitors. *Pflügers Arch.* **335**, 309–322.

KOSTYUK, P. G. & KRISHTAL, O. A. (1977). Separation of sodium and calcium currents in the somatic membrane of mollusc neurones. *J. Physiol.* **270**, 545–568.

KOSTYUK, P. G., KRISHTAL, O. A. & DOROSHENKO, P. A. (1975*a*). Outward currents in isolated snail neurones. I. Inactivation kinetics. *Comp. Biochem. Physiol.* 51C, 259–263.

KOSTYUK, P. G., KRISHTAL, O. A. & DOROSHENKO, P. A. (1975*b*). Outward currents in isolated snail neurones. II. Effect of TEA. *Comp. Biochem. Physiol.* 51C, 265–268.

LEE, K. S., AKAIKE, N. & BROWN, A. M. (1977). Trypsin inhibits the action of tetrodotoxin on neurones. *Nature, Lond.* **265**, 751–753.

MEECH, R. W. & STANDEN, N. B. (1975). Potassium activation in *Helix aspersa* neurones under voltage clamp: a component mediated by calcium influx. *J. Physiol.* **249**, 211–239.

MOORE, J. W. & COLE, K. S. (1963). Voltage clamp techniques. In *Physical Techniques in Biological Research*, vol. VI, ed. NASTUK, W. L. New York: Academic Press.

NARAHASHI, T., MOORE, J. W. & SCOTT, W. R. (1964). Tetrodotoxin blockage of sodium conductance increase in lobster giant axons. *J. gen. Physiol.* **47**, 965–974.

NEHER, E. (1971). Two fast transient current components during voltage clamp on snail neurons. *J. gen. Physiol.* **58**, 36–53.

NEHER, E. & LUX, H. D. (1973). Rapid changes of potassium concentration at the outer surface of exposed single neurones during membrane current flow. *J. gen. Physiol.* **61**, 385–399.

OKAMOTO, H., TAKAHASHI, K. & YOSHII, M. (1976*a*). Membrane currents of the tunicate egg under the voltage-clamp condition. *J. Physiol.* **254**, 607–638.

OKAMOTO, H., TAKAHASH, K. & YOSHII, M. (1976*b*). Two components of the calcium current in the egg cell membrane of the tunicate. *J. Physiol.* **255**, 527–561.

REUTER, H. (1973). Divalent cations as charge carriers in excitable membranes. *Prog. Biophys. molec. Biol.* **26**, 1–43.

ROBERGE, F. A., JACOB, R., GULRAJANI, R. M. & MATHIEU, P. A. (1977). A study of soma isopotentiality in *Aplysia* neurones. *Can. J. Physiol. Pharmac.* **55**, 1162–1169.

STANDEN, N. B. (1975). Voltage-clamp studies of the calcium inward current in an identified snail neurone: comparison with the sodium inward current. *J. Physiol.* **249**, 253–268.

THOMPSON, S. H. (1977). Three pharmacologically distinct potassium channels in molluscan neurones. *J. Physiol.* **265**, 465–488.

VAN DER KLOOT, W. & KITA, H. (1975). The effects of the 'calcium-antagonist' verapamil on muscle action potentials in the frog and crayfish and on neuromuscular transmission in the crayfish. *Comp. Biochem. Physiol.* **50**C, 121–125.

WALD, F. (1972). Ionic differences between somatic and axonal action potentials in snail giant neurones. *J. Physiol.* **220**, 267–281.